Supplementary Information (SI) for Journal of Materials Chemistry A.
This journal is © The Royal Society of Chemistry 2026

Supporting Information

Hexameric Structure-Dependent Catalysis of Oxalate Oxidase for Mitigating Shuttle Effect in High-Temperature Li–S Batteries

Tao Yang,[a] Peihang Li,[b] Yingxue Mei,[a] Dong Cai,[b] Chongju Chen,[a] Shuo Yang*[a] and Zhi Yang*[b]

a. College of Electrical and Electronic Engineering, Wenzhou University, Wenzhou, 325035, China

b. Key Laboratory of Carbon Materials of Zhejiang Province, Wenzhou University, Wenzhou, 325035, China

* E-mail: yangshuo@wzu.edu.cn (S.Y.), yang201079@126.com (Z.Y.)

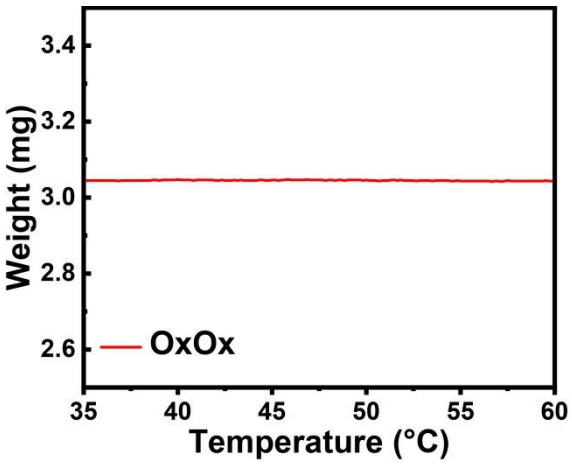

Fig. S1 TGA results of OxOx. Weight vs. temperature from 35 to 60°C.

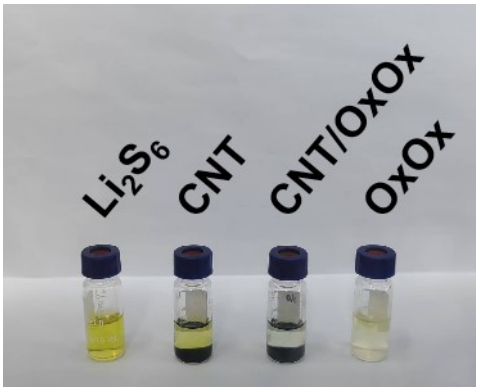

Fig. S2 Photographs of different materials in Li_2S_6 solutions.

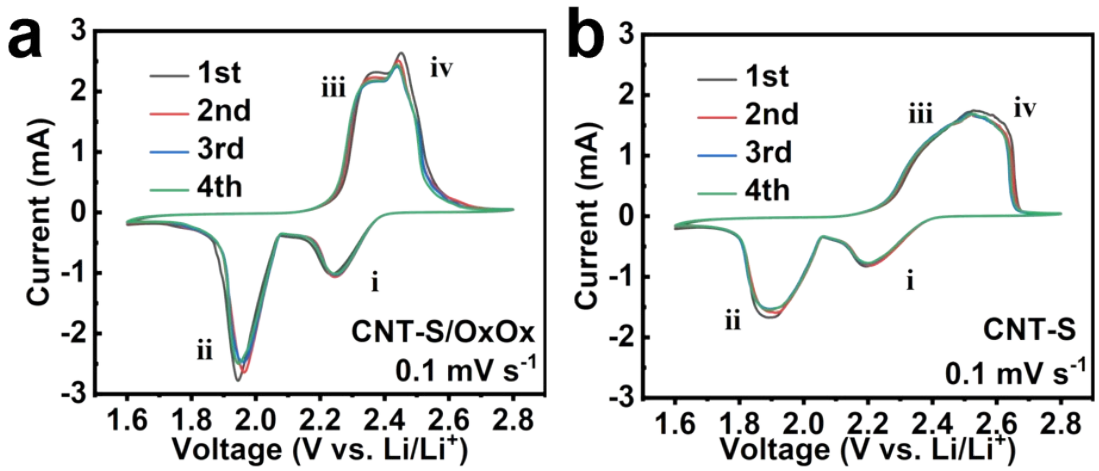

Fig. S3 CV curves of (a) CNT-S/OxOx and (b) CNT-S and cathodes at a scan rate of 0.1 mV s^{-1}.

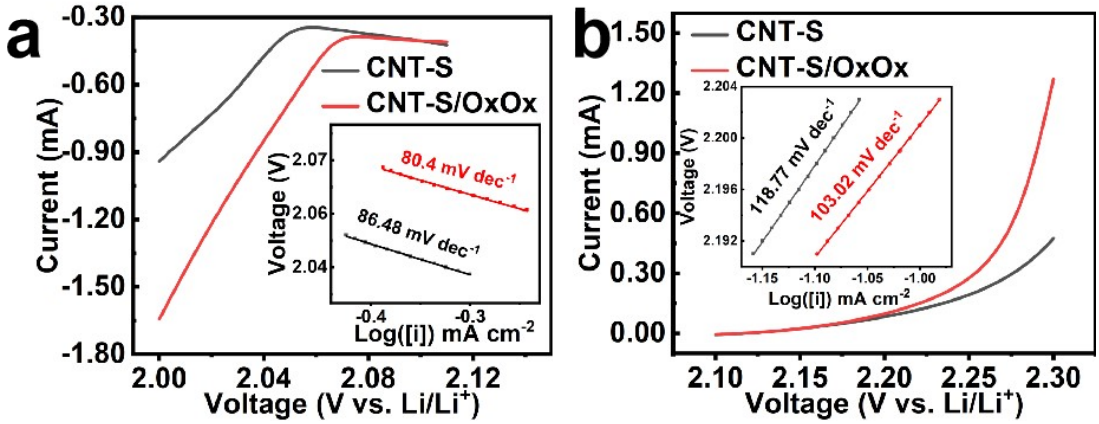

Fig. S4 The Tafel slope of the anodic processes obtained from the CV curves in Fig.1a correspond to (a) Peak ii and (b) Peak iii.

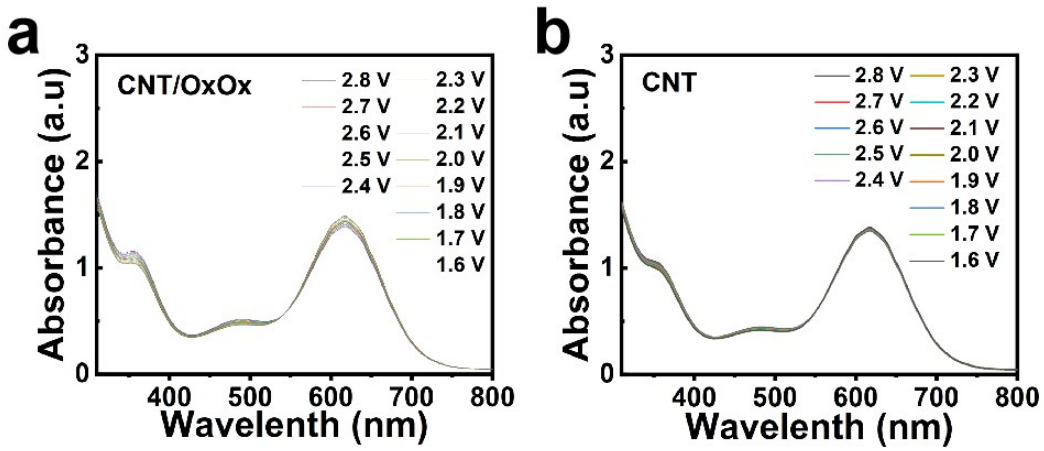

Fig. S5 In situ UV−vis absorption spectra of (a) CNT-OxOx and (b) CNT cathodes in Li_2S_8 and Li_2S_4 solution during the discharging process.

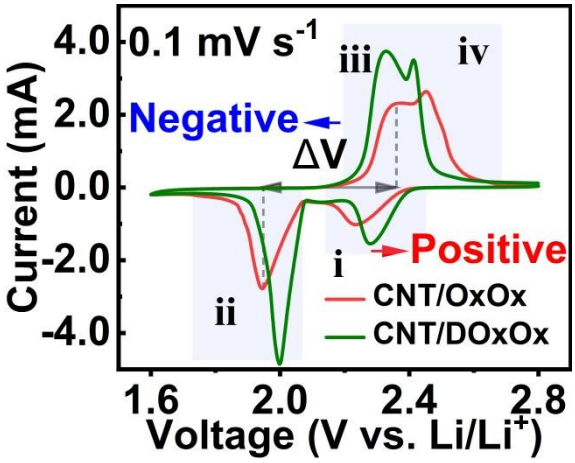

Fig. S6 CV curves of cathodes modified with 60°C heat-treated OxOx and DOxOx at 0.1 mV s^{-1}.

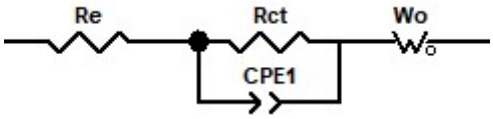

Fig. S7 The equivalent circuit model based on the Nyquist plots.

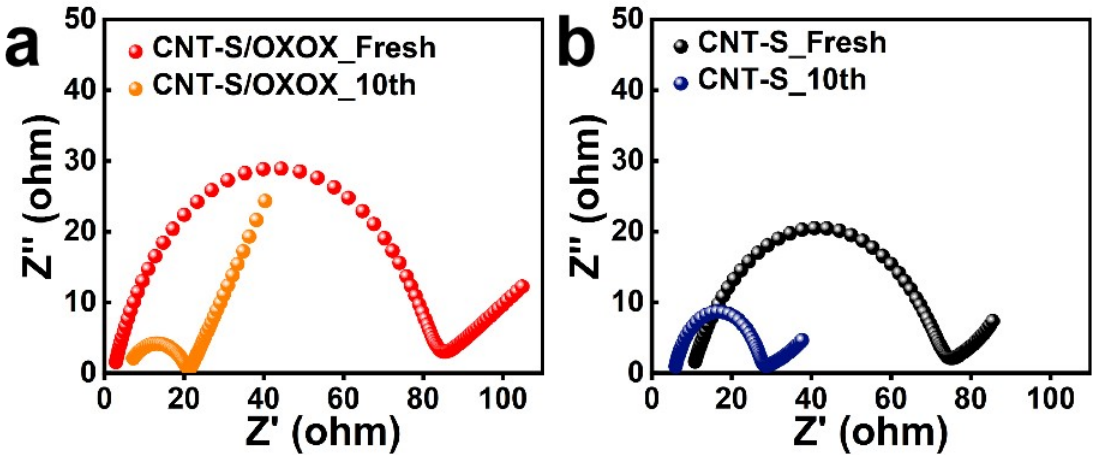

Fig. S8 The Nyquist curves for (a) CNT-S and (b) CNT-OxOx electrodes before and after cycling for 10 cycles.

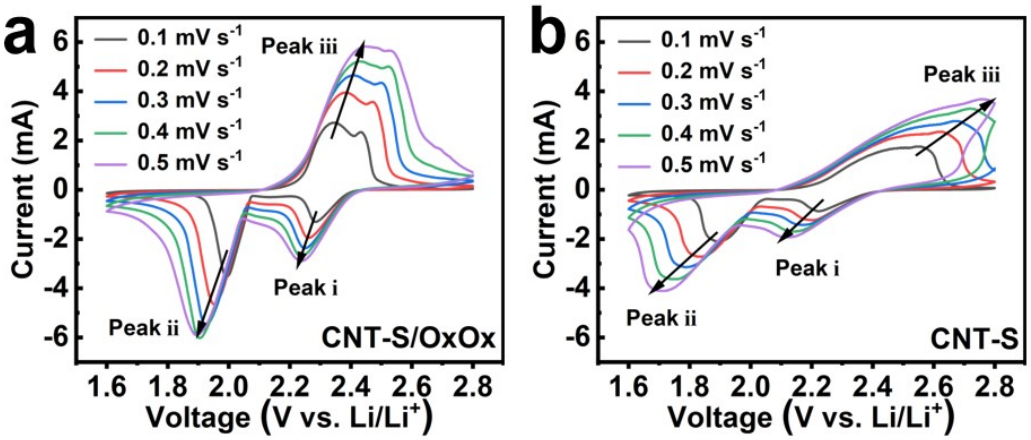

Fig. S9 CV tests at different scan rates. CV curves with scanning rates ranging from 0.1 to 0.5 mV s^{-1} using (a) CNT-S/OxOx, and (b) CNT-S cathodes.

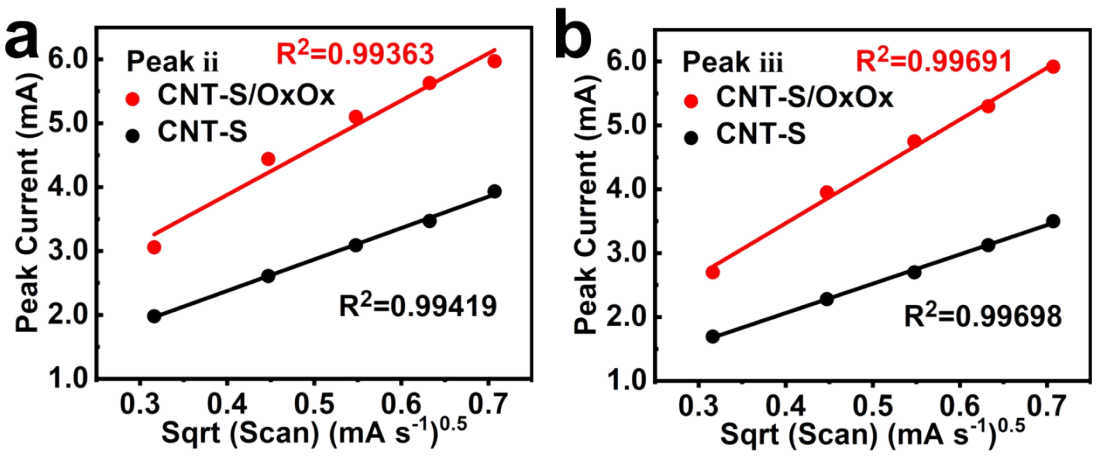

Fig. S10 The $I_p/v^{0.5}$ plot for (a) peak ii and (b) peak iii of CNT-S and CNT-S/OxOx derived from the CVs in Fig.S9.

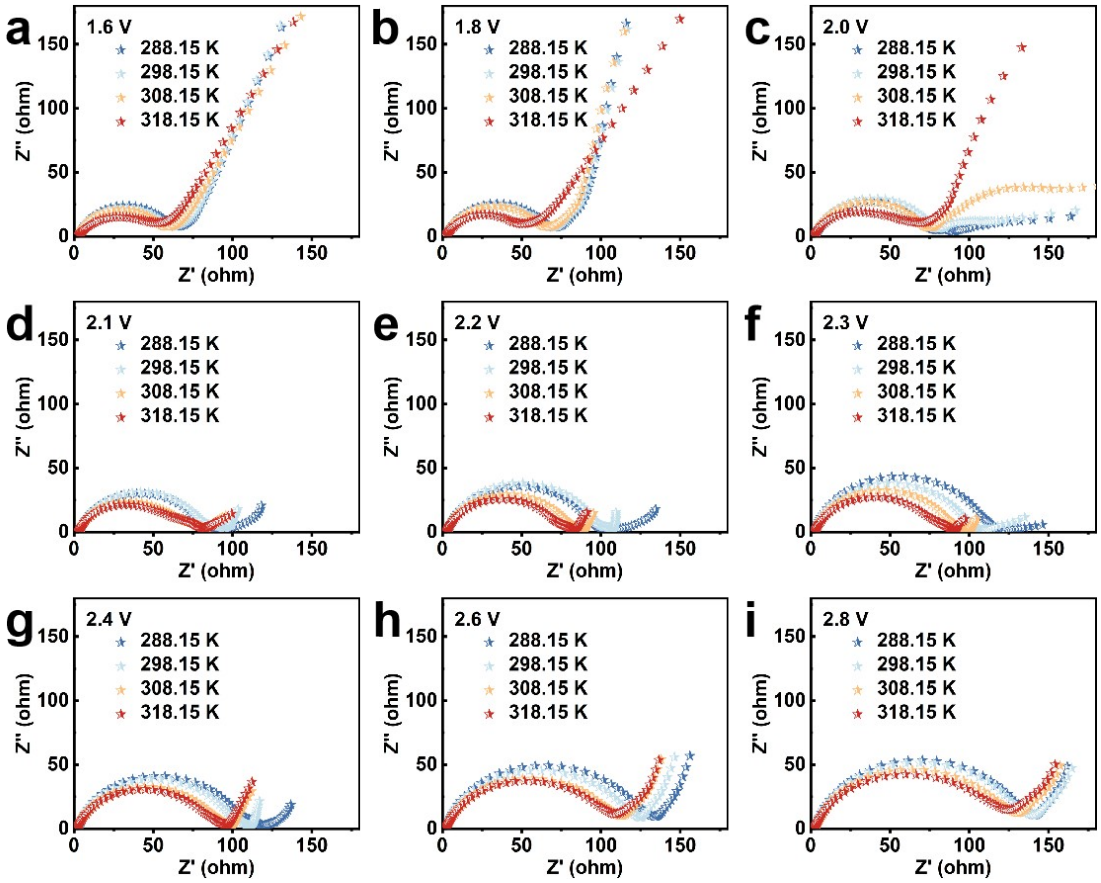

Fig. S11 The Nyquist plots of the CNT-S electrode at different temperatures and voltages during discharge process.

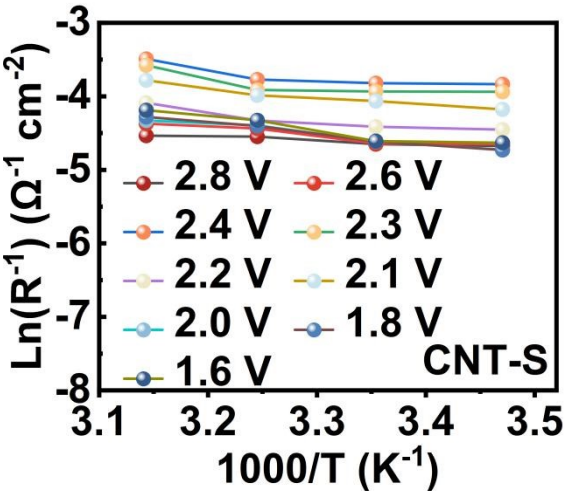

Fig. S12 The corresponding Arrhenius plots of the CNT-S electrode.

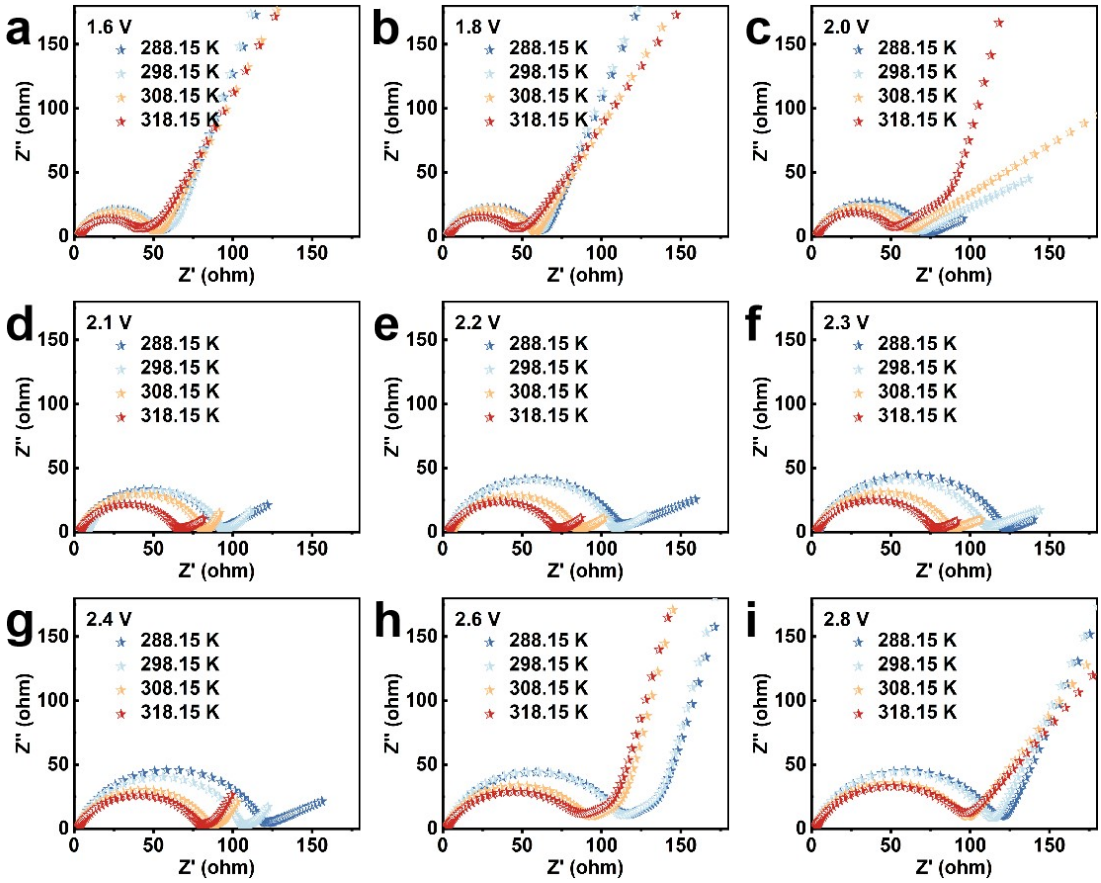

Fig. S13 The Nyquist plots of the CNT-S/OxOx electrode at different temperatures and voltages during discharge process.

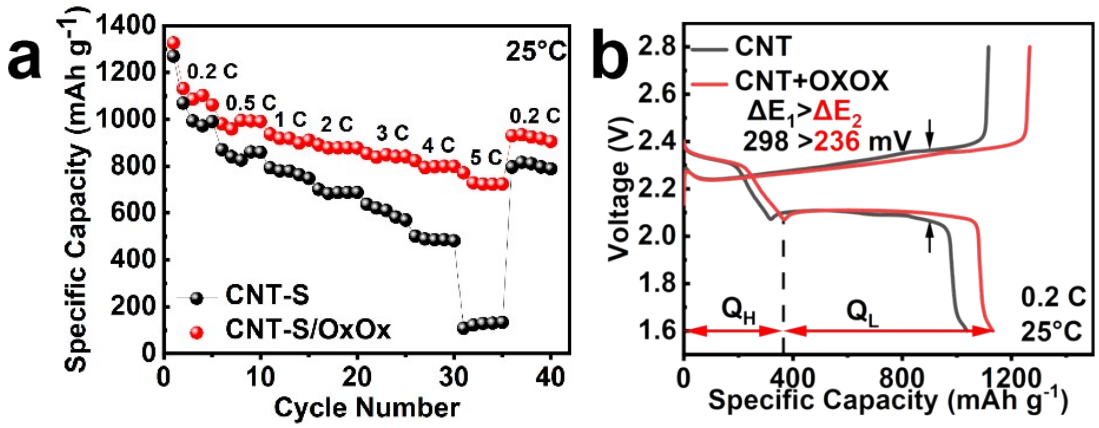

Fig. S14 (a) Rate capabilities of CNT-S and CNT-S/OxOx cathodes at 25 °C. (b) The 2nd-cycle galvanostatic discharge−charge curves at 25°C and 0.2 C.

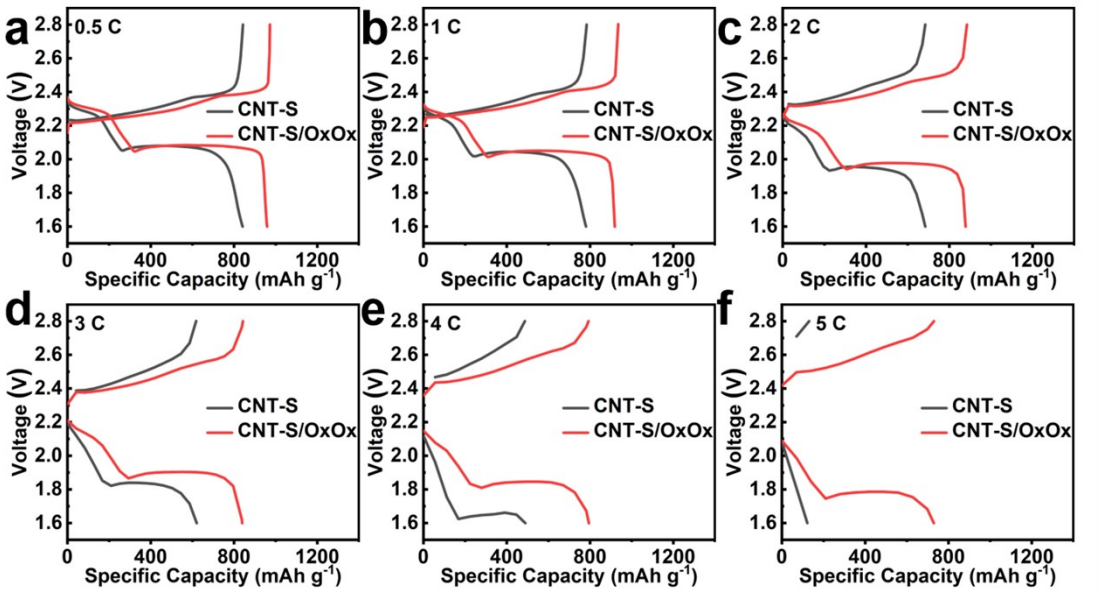

Fig. S15 The first-cycle galvanostatic charge-discharge curves of CNT-S and CNT-S/OxOx cathodes at (a) 0.5 C, (b) 1 C, (c) 2 C, (d) 3 C, (e) 4 C and (f) 5 C.

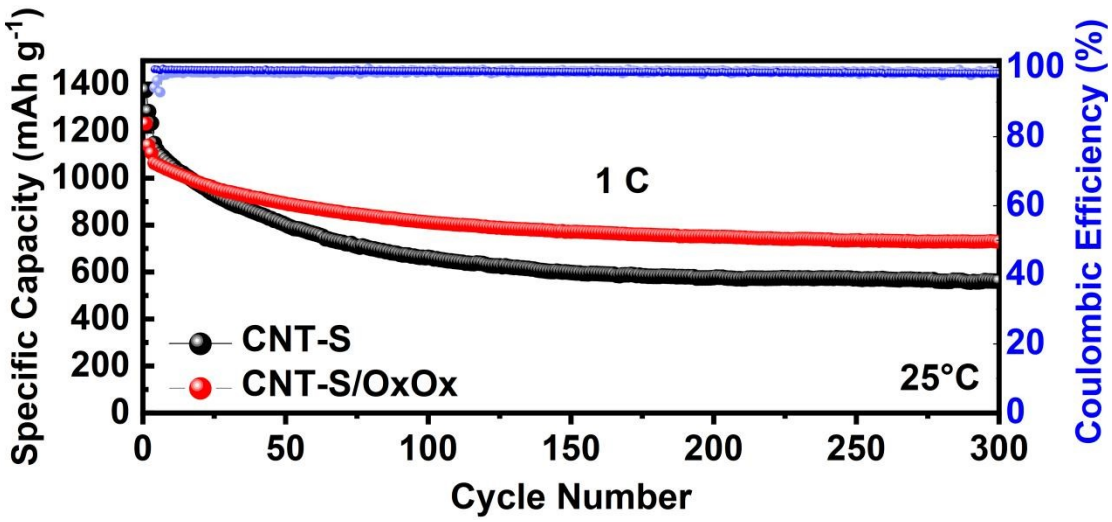

Fig. S16 Cycling performance of CNT-S and CNT-S/OxOx cathodes at 25°C and 1 C.

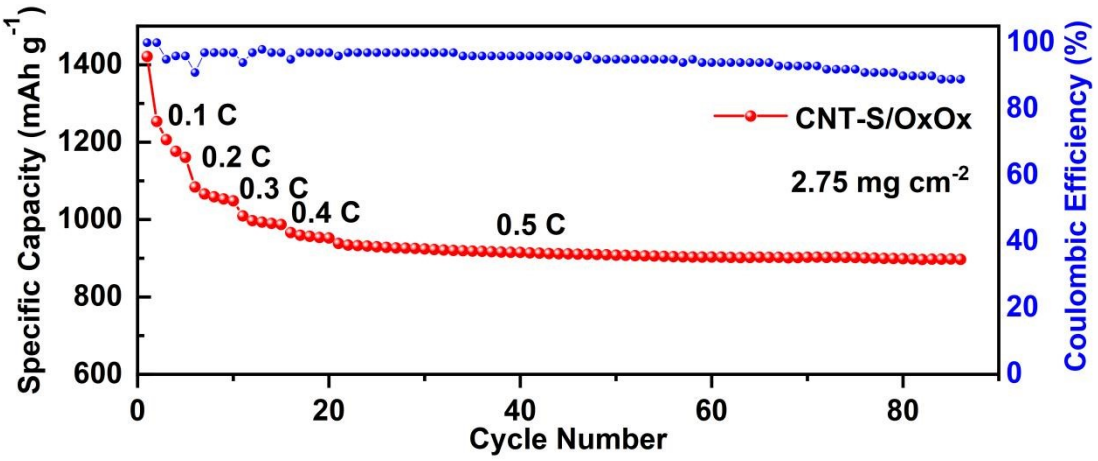

Fig. S17 Rate cycling performance of the CNT-S/OxOx electrode with a sulfur areal loading of 2.75 mg cm^{-2} at stepwise rates from 0.1 C to 0.5 C.

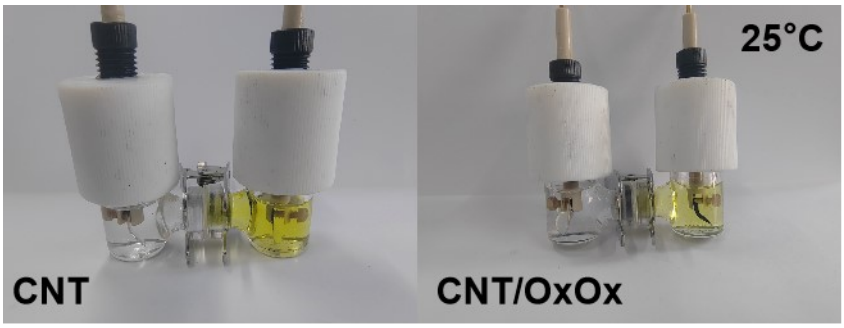

Fig. S18 Digital images of different electrodes after 1 h of discharge in an H-type cell at 25°C.

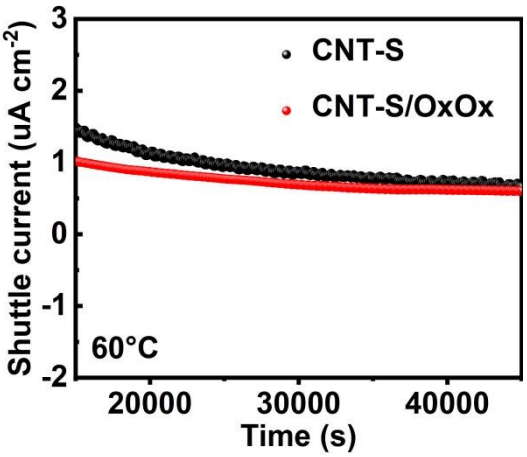

Fig. S19 Shuttle currents of Li−S coin cells with different cathodes at 60°C.

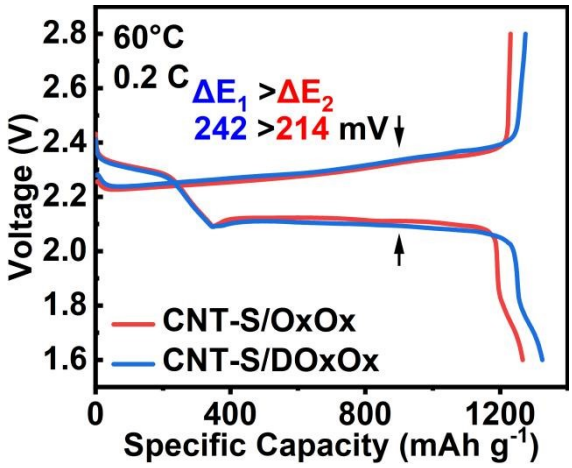

Fig. S20 The 2nd-cycle galvanostatic discharge−charge curves of CNT-S/OxOx and CNT-S/DOxOx electrodes at 60°C and 0.2 C.

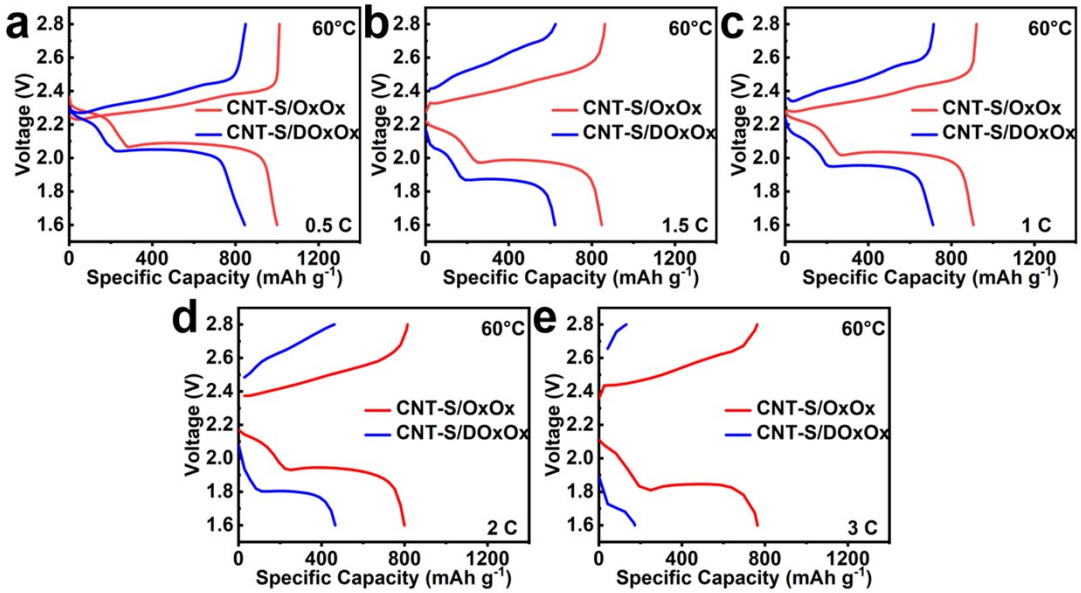

Fig. S21 The first-cycle galvanostatic charge-discharge curves of CNT-S/OxOx and CNT-S/DOxOx cathodes at 60°C: (a) 0.5 C, (b) 1 C, (c) 1.5 C, (d) 2 C, and (e) 5 C.

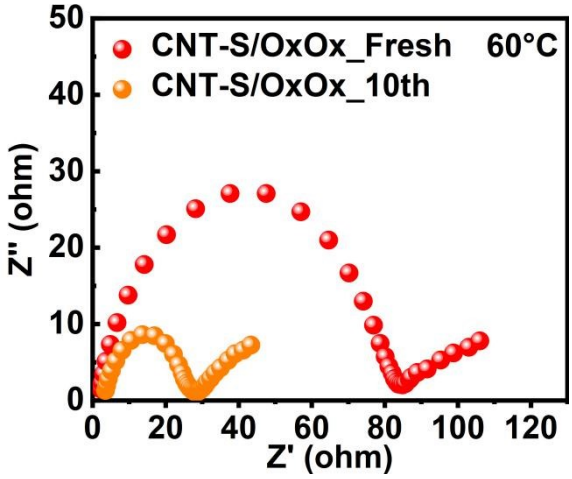

Fig. S22 The Nyquist curves for CNT-OxOx electrode before and after cycling for 10 cycles at 60°C.

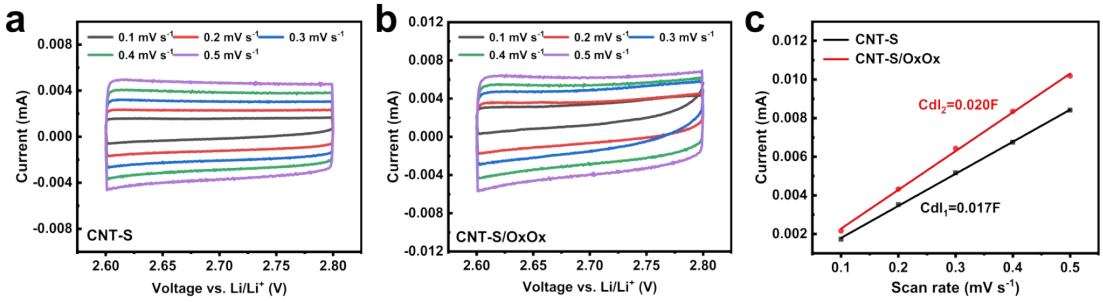

Fig. S23 CV curves of the (a) CNT and (b) CNT/OxOx cathodes tested in the non-faradic range. (c) Plots showing the C_{dl} for the two cathodes.

Table S1 Comparison of high-temperature electrochemical performance of Li-S batteries with different modification strategies.

Material	Initial rate capabilities [mAh g^{-1}]	Rate capability [C]	T [℃]	Cycle Number	Ref
W-VO_2(R)	1065.9	0.2	50	120	1
PPy/S/MWCNT	1000	0.5	75	50	2
C/S PAl	800	0.1	60	50	3
C/SnO_2/S	1161	1	60	100	4
RGO/hBN/S	132.48	1	110	50	5
Co_3O_4-350/PI/LLZO	1500	0.1	80	200	6
CNT−S/OxOx	1064.68	1	60	300	This work

References:

1. G. Liu, Q. Zeng, S. Tian, X. Sun, D. Wang, Q. Wu, W. Wei, T. Wu, Y. Zhang and Y. Sheng, *Small*, 2024, **20**, 2307040.
2. M. Kazazi, *Ionics*, 2016, **22**, 1103–1112.
3. Y. Peng, Z. Peng, Y. Qiu, K. Yan and G. Wang, *Journal of Energy Storage*, 2020, **27**, 101104.
4. C. Wang, G. Wang, Q. Xiao, X. Yang, H. Yan, J. Qi, S. Liu, J. Wang and Y. Zhang, *Electrochim. Acta*, 2024, **487**, 10.
5. Y. Mussa, Z. Bayhan, N. Althubaiti, M. Arsalan and E. Alsharaeh, *Materials Chemistry and Physics*, 2021, **257**, 123807.
6. Z. Zhou, Y. Li, T. Fang, Y. Zhao, Q. Wang, J. Zhang and Z. Zhou, *Nanomaterials*, 2019, **9**, 1574.